DEVICE TRANSPLANT OF OPTICAL MEMS FOR OUT OF PLANE BEAM STEERING

Hung Nguyen, John Guo-Dung Su, Hiroshi Toshiyoshi, and Ming C. Wu

Tel: (310) 825-6859, Email: wu@ee.ucla.edu
Department of Electrical Engineering, University of California at Los Angeles
66-147D Engineering IV Building, Los Angeles, CA 90095-1594

ABSTRACT

We report on a substantially improved process for which an array of optical MEMS devices (MOEMS) are batch transferred onto a quartz wafer such that through wafer beam scanning can be achieved. MEMS optical scanners are successfully fabricated, transferred, and actuated for out-of-plane beam steering. DC transfer curves of control devices on silicon and those transferred on quartz exhibit similar pullin voltages of 135 V and 142 V respectively. Similarly, resonance for control device peaked at 1.1 kHz while transferred devices exhibit higher resonance at 1.2 kHz.

INTRODUCTION

With the advent of surface-micromachining, many optical MEMS devices can be fabricated with nearly three-dimensional features. Moreover, standard surface micromachining allows various films to be used as structural and sacrificial layers. Accordingly, an entire optical bench including lenses, optical switches and scanners can be fabricated monolithically on a single cm^2 chip [1]. Commercial silicon-based foundries provide an additional benefit of a low cost alternative to MEMS fabrication.

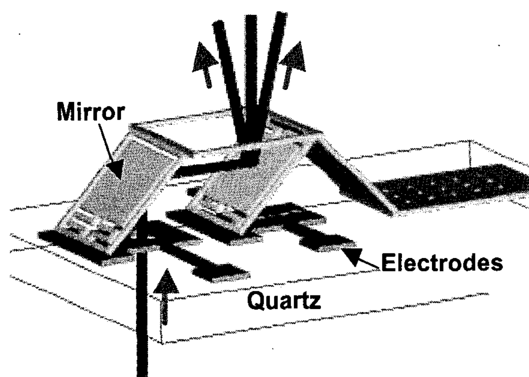

Figure 1. *Schematic diagram of cascading optical scanner*

Numerous variations of optical scanners have been fabricated by surface micromachining—each having its own advantage and limitations. One such scanner employs a gimbal design, which allows two-dimensional rotation of the center mirror and frame on a single platform [2]. While this design offers the benefits of compactness and reduction in drift of the reflected light, it inevitably suffers from cross-talk as its axes of rotation are coupled. Two separate one-dimensional scanners operating in unison can perform equally well without cross-talk [3]. However, incident light is always parallel of the substrate limiting the size of arrays on a single chip without obstructing the light path.

We have designed and fabricated an optical scanner using a standard silicon micromachining process as shown in Fig. 1. This electrostatically driven MEMS scanner consists of two cascading mirror actuators with each controlling one axis of rotation. Unlike previously mentioned scanners, scanning with this device is performed normal to the surface thereby allowing a larger array of scanners without any obstruction. Furthermore,

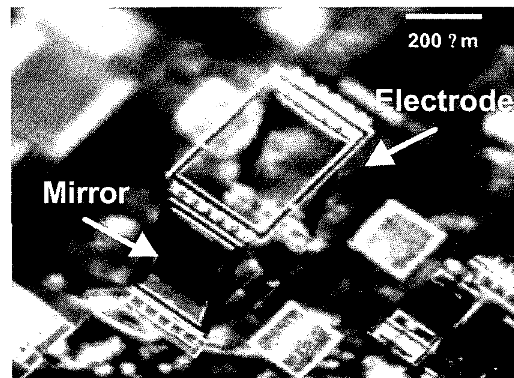

Figure 2. *Microscopic image of transferred optical scanner on quartz substrate*

this scanner relies on transmission through the substrate. However in its present form, the scanner cannot operate efficiently. Because it requires through-wafer beam scanning, the use of silicon as the host wafer in many MEMS processes is highly undesirable due to its high absorption, especially in the visible range.

Some have proposed etching through the entire (111) silicon wafer to create an optical path to the MEMS devices from the back of the wafer [4]. Others have opted for transferring devices using photoresist-assisted bonding [5]. There also have been recent developments in batch transfer of RF devices with the use of gold-gold compression bonding [6,7]. However, the authors reported that precise pressure and

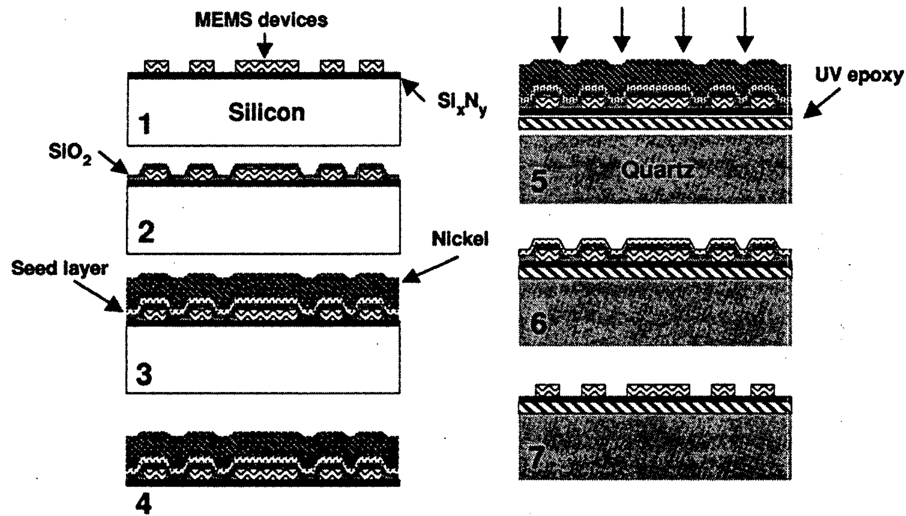

Figure 3. *Wafer transfer process flow*

alignment during bonding are critical due to its affect of the final height between electrodes and device. Hence, we propose an improved wafer-scale MEMS transplant of an entire chip onto a new substrate [8]. This process allows us to design and fabricate our optical scanners by a standard process and batch transferring these devices onto quartz such that through-wafer beam scanning can be achieved for a wider range of wavelengths. A microscopic image of a transferred MEMS optical scanner on a quartz substrate is shown in Fig. 2.

PRINCIPLE AND DESIGN

The MEMS optical scanner is fabricated using the Multi-User MEMS Processes (MUMPs) foundry. This process includes phosphosilicate glass (PSG) as the sacrificial layer. Three layers of polysilicon compose the structural components of the MEMS devices. A thin layer of Cr/Au (500 nm) is used as metallization. The MEMS scanner consists of two independently driven mirror actuators. The mirrors have an area of 200x200 μm^2 with a thickness of 1.5 μm. As in Fig. 1, both mirrors are assembled simultaneously into its final 45-degree position and are attached to polysilicon frames by 1.5 μm-thick polysilicon springs. Each actuator controls either horizontal or vertical scan. The first electrode is designed to have a 50-μm diameter hole to allow the transmission of the light from below the substrate. With a transparent substrate, the light can transmit through the wafer and reflect onto both mirrors. By actuating the mirrors simultaneously, two-dimensional scanning can be achieved.

FABRICATION

Our wafer-scale device transfer technique has been previously reported however, drastic improvements have recently been made to increase device yield and reduce fractures and stress gradients as described in Fig. 3. As before, a 1-μm-thick oxide layer is deposited by PECVD to passivate the device layers. A Ti-Ni (400 Å/1000 Å) seed layer is sputtered over the sample. A 70-um-thick nickel layer is electroplated onto the sample. A clean seed layer is necessary for ideal plating. This requires an etch in diluted hydrochloric acid solution. Poor adhesion between the seed layer and plated nickel occurs without proper cleaning. The plated nickel layer reduces the surface topography and hence, lessens the effects of stress gradients that may occur during bonding. In fact, the nickel is sufficiently rigid to keep the membrane intact as seen in Fig. 4. Stresses during the process can lead to fractures over the entire device layers once the sample is released in hydrofluoric acid. The sample is mounted onto a lapping plate where the silicon substrate is removed by a combination of a mechanical lap and a XeF_2 chemical etch. To ensure complete bonding, the surface of the device membrane must be free of particles. Since, the XeF_2 etch leaves silicon-based debris, potassium hydroxide (KOH) is

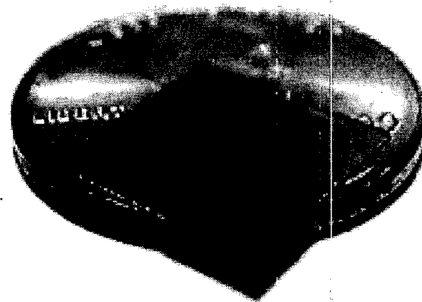

Figure 4. *Device membrane held by thick (70 ?m) electroplated nickel*

used as a freckle-etch to remove all undesirable contaminants. A new quartz substrate is attached to the membrane with UV epoxy. Pressure is applied over the entire sample while the epoxy is being cured. The devices with the new quartz substrate are removed from the lapping plate and immersed in nickel etchant. Final release of the devices involves the removal of both titanium seed layer and phosphosilicate glass (PSG) sacrificial layers in hydrofluoric acid (HF).

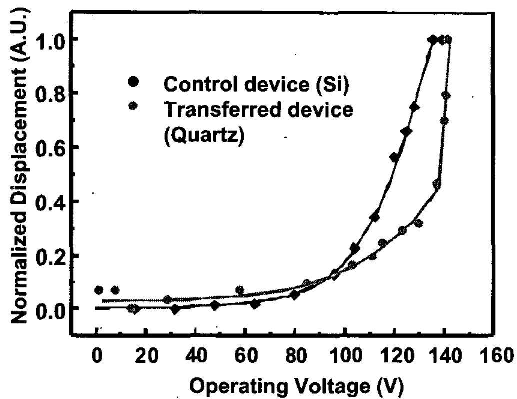

Figure 5. *DC transfer curves for control and transferred optical scanners*

MEASUREMENTS

To demonstrate the feasibility of this batch transfer process, several electrostatic and mechanical analysis were performed on the scanner. A DC transfer curve is obtained for MEMS devices on both the original silicon and quartz substrates as shown in Fig. 5. A laser Doppler monitor (LDM) and He-Ne laser was used to assist in the measurement of the mirror displacement as a sinusoidal signal of 200 Hz was applied to the actuator. The pullin voltage was found at approximately 142 V for the transferred device. This value is comparable to that of the control scanner (135 V). Factors including exact height of the mirror with respect to its electrode can affect the outcome of the pulling voltage.

Figure 6 shows the frequency response of both devices. Resonance frequency was found by using the same LDM. The scanner was driven at an AC voltage of 63 V. The mirror deflection peaked at approximately 1.2 kHz for the transferred scanner. The control scanner on its original silicon substrate exhibits a resonance at 1.1 kHz. Normalization of the dynamic response and transfer curves is needed as the position of the beam spot of the LDM on the mirror affects the magnitude of the displacement.

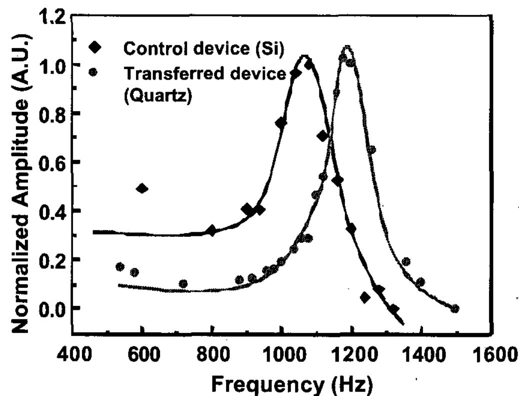

Figure 6. *Dynamic response*

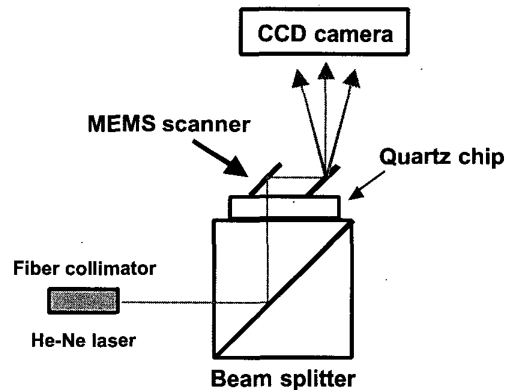

Figure 7. *Schematic diagram of line-scan experiment*

A CCD camera was also used to capture the image of the reflected He-Ne light. For this experiment, we analyzed a slightly modified version of the aforementioned optical scanner. Figure 7 shows the setup of the experiment. The quartz sample is mounted onto a beam splitter. The CCD camera is positioned just above the MEMS scanner. The He-Ne light is reflected onto the beam splitter and transmitted through the quartz substrate onto the mirror actuators of the scanner. Figure 8 includes a collage of several stroboscopic video images of the beam spot as it traverses along the length of the CCD camera. From the data collected by the camera, it is determined in Fig. 8 that there are no major shifts in resonance at various operating voltages between 64 and 107 V. Furthermore, the maximum scanning angle is roughly ±13 degrees.

In addition to the scanner's performance, the nitride and epoxy films were also characterized by examining micro-bridges, which measures contractions from the bottom films. From the buckling of these doubly clamped beams shown in Fig. 9, the nitride and bonding layer exhibit contractions of 0.135-μm for a 300-μm length. This translates to a 0.045% shrinkage. More analysis must be done to determine the contribution of each film to the stress found in the micro-bridges.

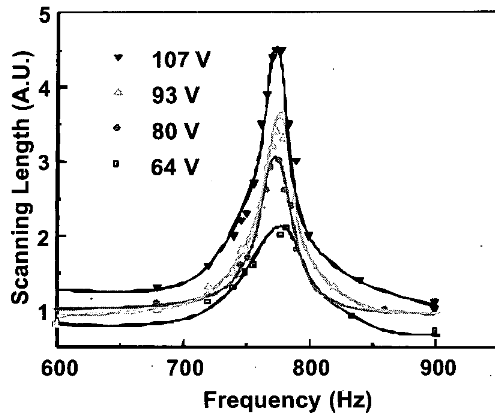

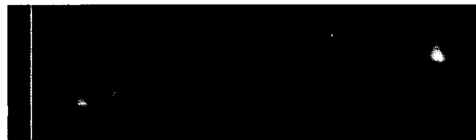

Figure 8. *Stroboscopic images of line scan and frequency response at various voltages*

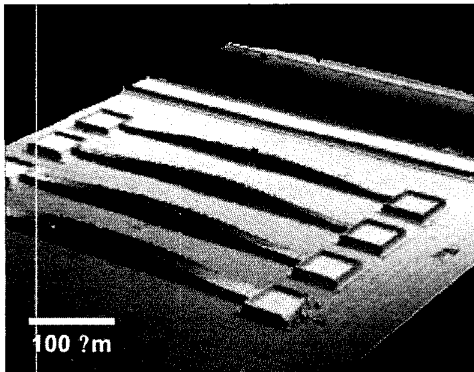

Figure 9. *Surface profiles of micro-bridges*

CONCLUSION

To facilitate the need for beam steering through the wafer, an MEMS optical scanner is successfully transplanted onto a quartz substrate. Presently a one-dimensional line scan is obtained. We have also examined the scanners' static and dynamic responses to demonstrate the feasibility of this process. The transferred scanner shows a pullin voltage of 142 V and resonance at 1.2 kHz without significant resonance shift. With this success, other optical MEMS devices can potentially benefit from this technology. We envision employing wafer transfer on other MOEMS devices such as diffractive lenses, tunable gratings, and micro-shutters.

Acknowledgement

The authors like to thank Pam Patterson, Paulo Motta, Henry Yang, and Patrick deGuzman for their valuable discussion on nickel electroplating.

REFERENCES

[1] Lin, L.Y.; Lee, S.S.; Pister, K.S.J.; Wu, M.C., *IEEE Photonics Technology Letters*, Dec. 1994, p.1445-7.

[2] Fan, L.; Wu, M.C., *IEEE/LEOS Summer Topical Meeting,* 1998, p.II/107-8.

[3] Conant, R.; Hagelin, P.; Krishnamoorthy, U.; Solgaard, O.; Lau, K.Y.; Muller, R.S., *Proc. of the 10th Int. Conf. on Solid-state Sensors and Actuators (Transducers '99),* p.2D-3.2, 1999

[4] Sadler, D.J.; Garter, M.J.; Ahn, C.H.; Koh, S.; Cook, A.L, *Journal of Micromechanics and Microengineering,* vol.7 (no.4), p.263-9, Dec. 1997

[5] T. Akiyama, U. Staufer, and N. Rooij, *IEEE Journal of Microelectromechanical Systems,* pp. 65-70, 1999

[6] Milanovic, V; Maharbiz, M; Singh, A, Warneke, B; Zhou, N; Chan, H; and Pister, K.S.J, *Proceedings IEEE Thirteenth Annual International Conference on Micro Electro Mechanical Systems,* Miyazaki, Japan, 23-27 Jan. 2000, p.787-92.

[7] Feng, Z.; Zhang, H.; Zhang, W.; Su, B.; Gupta, K.C.; Bright, V.M.; Lee, Y.C., *Tech. Digest Solid-state Sensor and Actuator Workshop (Hilton Head 2000)*, p. 255, 2000

[8] Nguyen, H.; Patterson, P.; Toshiyoshi, H.; Wu, M.C., *Proceedings IEEE Thirteenth Annual International Conference on Micro Electro Mechanical Systems,* Miyazaki, Japan, 23-27 Jan. 2000, p.628-32.